

## Transformations in WC lattice and polytype formation in the process of sintering of W/C<sub>60</sub> mixture



I.A. Perezhogin<sup>a,b,\*</sup>, B.A. Kulnitskiy<sup>a,c</sup>, A.E. Grishtaeva<sup>a,c</sup>, S.A. Perfilov<sup>a</sup>, R.L. Lomakin<sup>a</sup>, V.D. Blank<sup>a,c</sup>

<sup>a</sup> Technological Institute for Superhard and Novel Carbon Materials, Centralnaya str. 7a, Troitsk 142190, Moscow, Russian Federation

<sup>b</sup> International Laser Center, Lomonosov Moscow State University, Leninskie Gory 1, Moscow 119991, Russian Federation

<sup>c</sup> Moscow Institute of Physics and Technology State University, Institutskiy per. 9, Dolgoprudny 141700, Moscow, Russian Federation

### ARTICLE INFO

#### Article history:

Received 6 June 2014

Accepted 4 August 2014

Available online 10 August 2014

#### Keywords:

Tungsten carbide WC

Sintering

HRTEM

Polytype

Stacking fault

### ABSTRACT

WC nanoparticles having size from nanometers to tens of nanometers surrounded by amorphous carbon and onion-like carbon structures were obtained by milling W/C<sub>60</sub> mixture and subsequent sintering by short pulse of electric current. We performed transmission electron microscopy studies of the obtained sample. Almost all of the WC nanoparticles possessed stacking faults in {100} planes stacking. It is known from scientific literature, that such a stacking fault is equivalent to the rotation of the tungsten carbide cells at 90° in the plane of the defect, and it favors the formation of  $\Sigma = 2$  boundary between the grains of WC, rotated at 90° relatively to each other. In a big number of nanoparticles in our sample we observed such an orientation of the neighboring grains. Sometimes a single nanoparticle consists of several grains having  $\Sigma = 2$  and higher  $\Sigma$  boundaries. Also we observed polytype in WC not reported earlier, appearing due to the consequence of stacking faults in (100), and we propose the structure of this polytype. We believe, that the formation of polytypes and  $\Sigma = 2$  and higher  $\Sigma$  boundaries took place during the sintering of W/C<sub>60</sub> mixture and happened due to the specific features of the tungsten carbide formation and carbon diffusion through the tungsten.

© 2014 Published by Elsevier Ltd.

### Introduction

At the present time tungsten carbide WC is one of the most promising and most available hard materials, which are widely used in industry and science. It is known that the efficient use of the mechanical properties of WC can be achieved when its particles are embedded into the “matrix” of softer material (see, for example, [1] or earlier works). At the present time WC–Co composition is most known and most widespread. However, other metals are also frequently used for the formation of hard composites and coatings. Disadvantages of Co as binding material are its relative toxicity and higher cost compared with alternative materials such as Fe–Ni or Ni–Fe–Cr alloys. The possibility of the usage of the latter two is under consideration at the present time [1].

One of the important problems accompanying the sintering of WC–Co mixture is the growth of WC nanocrystals in size. It is known that big particles in this composition represent its “weak” points, since they serve as the origins of cracks under loading [2]. The smallest size of the tungsten carbide nanoparticles embedded in Co matrix achieved up to date is somewhat below the 100 nm [3].

In view of these problems the usage of a new binding material is highly relevant for the production of WC-based composition with improved properties. C<sub>60</sub> fullerene is very promising material for a “matrix” in this composition. It is known [4] that under conditions of high pressure and high temperature there can be obtained compositions with very high values of elasticity modulus and hardness from C<sub>60</sub> used as precursor. In addition to this, the usage of carbon material makes it possible to synthesize tungsten carbide in course of sintering tungsten nanopowder with carbon material, which, in its turn, can be useful to limit the undesirable process of WC grain growth.

Apart of this, the structure of the obtained WC nanoparticles represents special interest. Different defects in WC crystal lattice can remarkably affect strength and durability properties of the WC–Co composition. In particular, stacking faults in {100} planes in WC weaken the composition, while the stacking faults in (001) planes favor the growth of the nanocrystal WC platelets perpendicular to [001], which improves the mechanical properties of WC–Co, because WC elastic properties are anisotropic [2,5,6].

The main goal of our work is to find possible ways of creation of the prospective materials based on WC and C<sub>60</sub>. In order to study such process we perform pulsed sintering of W nanopowder with C<sub>60</sub>, and then study the sample in transmission electron microscope (TEM) in order to characterize the structure of the obtained composition and crystal lattice defects in WC nanoparticles.

\* Corresponding author at: Technological Institute for Superhard and Novel Carbon Materials, Centralnaya str. 7a, Troitsk 142190, Moscow, Russian Federation.

E-mail address: [i.a.perez@gmail.com](mailto:i.a.perez@gmail.com) (I.A. Perezhogin).

## Experimental

In order to obtain tungsten carbide nanopowder by means of tungsten carburization under high pressure we used a precursor consisting of tungsten powder (1–3  $\mu\text{m}$  grain size) and 99.5% purity fullerene  $\text{C}_{60}$  (20.4 wt.% of  $\text{C}_{60}$  and 79.6 wt.% of W, or 75 and 25 vol.% of  $\text{C}_{60}$  and W correspondingly). First, the mixture was placed into a planetary ball mill made of WC material in a glove box in Ar atmosphere. The mixing and the milling of the powders were carried out there during 20 min with an acceleration of 30 g. Afterwards the mixture was compacted into cylindrically shaped samples with a diameter of 8 mm and 5 mm height. In order to heat such a sample by the electric current pulse at tension about 5–10 V with the release of heat power of about 8–20 kW it is necessary to provide the resistance of the sample not higher than  $10^{-5}$ – $10^{-4} \Omega \cdot \text{m}$ . Since the fullerene is practically isolating material under such conditions, it is necessary to have enough tungsten nanoparticles in the mixture so they can form conducting chains. It was established experimentally that necessary amount of tungsten is about 25 vol.%.

During the sintering the pressure in the chamber was 7.7 GPa for the pulse power 9 kW and the pulse duration 0.4 s. Further the initial tungsten nanopowder, the milled mixture of tungsten and  $\text{C}_{60}$ , and the sintered sample were examined in TEM. TEM studies were performed on JEM-2010 at 160 kV accelerating voltage with a GIF Quantum attachment for electron energy loss spectroscopy (EELS) and with an EDS attachment.

### General results of the TEM observation

TEM examination of the milled mixture before the sintering has shown that the characteristic size of the nanoparticles was ranging from nanometers to tens of nanometers, and most of them were not faceted. Most of the particles were pure tungsten or various tungsten oxides. The presence of oxides can be explained by the admixture of accident amounts of oxygen into the powder during the milling and its subsequent reaction with tungsten nanoparticles (oxides were absent in the origin powder). The carbon in the sample presented mainly as the fragments of fullerene face-centered cubic (FCC) lattice.

Afterwards we studied the sample obtained after the sintering of the milled powder. Carbon in the sample partially transformed into closed onion-like curved structures (consisting of few layers) and partially into amorphous carbon. Tungsten presented as WC nanoparticles having the size of the same order as in the milled sample (from nm to tens of nm). Almost all of the WC particles possessed crystal lattice defects. Microdiffraction analysis and high resolution TEM (HRTEM) image analysis have shown that these defects are the stacking faults in  $\{100\}$  planes.

### Discussion of results

Basing on the obtained TEM data we conclude that only the mixing and fragmentation of W and  $\text{C}_{60}$  took place in a ball mill during the milling without the formation of tungsten carbide. Tungsten nanoparticles have lost their faceted shape in this process. Some of the nanoparticles also were oxidized due to the admixture of minute amounts of oxygen to the sample. Afterwards during the sintering the reaction of tungsten oxides and carbon took place with the reduction of tungsten oxides (such reaction is also described in [7] under analogous conditions). Also carbon reacts with pure tungsten with the formation of tungsten carbide WC. The excess carbon, which did not take part in any of the abovementioned reactions transform into amorphous carbon or into the closed onion-like curved structures during the sintering.

WC crystal lattice is hexagonal one, and its cell has basic vectors  $a = b = 0.291 \text{ nm}$  and  $c = 0.284 \text{ nm}$ . The main “building” element of its lattice is a trigonal prism of tungsten atoms (Fig. 1) with a carbon atom in the center of the prism. Therefore, each tungsten atom is

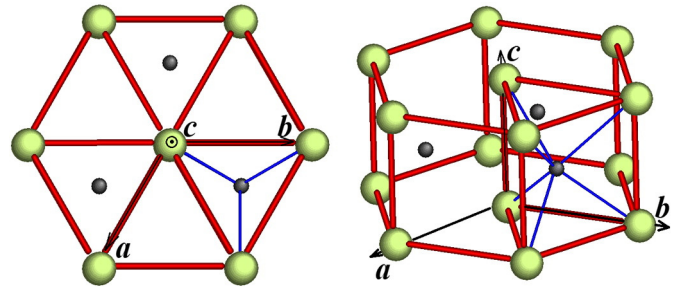


**Fig. 1.** The scheme of WC crystal lattice cell. Black spheres are carbon atoms and gray (green) spheres are tungsten atoms. The main “building” element of its lattice is a trigonal prism of tungsten atoms with a carbon atom in the center. In other words, the lattice can be represented as superposition of trigonal prisms composed by carbon and tungsten atoms shifted one relatively to another. The lateral facets of these prisms are almost squared ( $a \approx c$ ). (For interpretation of the references to color in this figure legend, the reader is referred to the web version of this article.)

connected with 6 carbon atoms and vice versa. Each lateral facet of such prism represents a rectangle which sides ( $a$  and  $c$ ) have relative difference less than 0.3%. Thus, the lateral facets of the prism are practically squared.

It was shown in [8,9] and earlier works, that the stacking faults observed in our sample represent itself a shift of the atomic planes (100) at vector  $1/2^* [011]$  (Fig. 2a). As a result of such a shift the triangular prisms of WC rotate at  $90^\circ$  in a layer where the stacking fault has occurred (Fig. 2b). Such a defect requires minimum of energy since in this case the amount and the lengths of the bonds between carbon and tungsten atoms remain the same within the stacking fault layer [8].

In the high resolution image in Fig. 3 there are stacking faults in  $\{100\}$  planes seen in a WC nanoparticle. In places, where these stacking faults are many, they are seen as bands, and there appears a contrast of another atomic planes perpendicular to the band, which can be treated as (001), since their interplanar distance 0.28 nm corresponds to (001). (The interplanar distance and the orientation of the fringes in this band were studied by the Fourier analysis of the image).

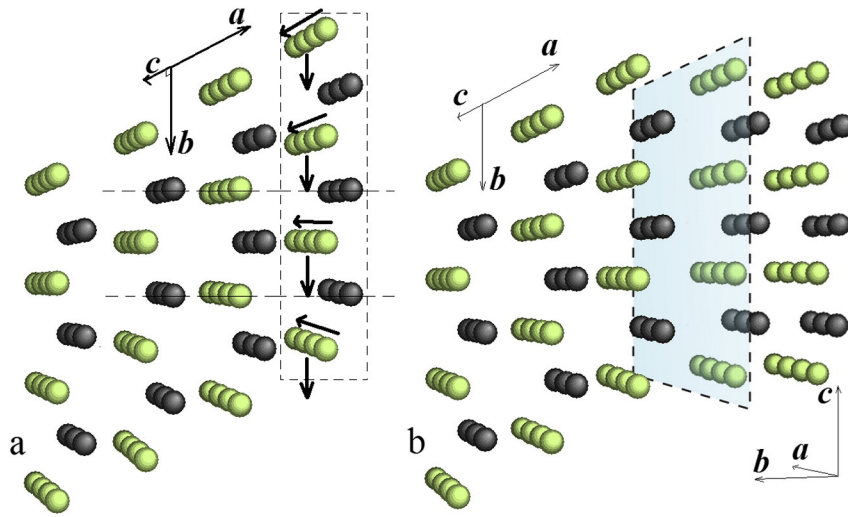
However, (001) does not belong to the zone axis [001]. Their appearance is due to the formation of the lattice layer with the zone axis [010] in this band, which is build by a consequent stacking faults in (100) planes of initial (right lower part) crystal (as in Fig. 2b). These stacking faults can appear both after the formation of the nanoparticle or during the reaction between tungsten and carbon.

Fig. 4 shows a particle where relatively big fragments of WC lattice are rotated one relatively to another at  $90^\circ$  connected by grain boundaries with different  $\Sigma$ . In this case most probably the formation of these fragments took place during the growth of the particle.

Apart of this we found polytypic structure in WC. Fig. 5 shows a characteristic example of this polytype. There is a particle with big amount of stacking faults in it. Areas “1” have [001] zone axis while areas “2” have [010] zone axis. Boundaries of these areas are parallel to (100) (which has the same orientation in both types of areas) and perpendicular to (001) in “2”.

However, there are also areas “3”, where another type of contrast is seen, which cannot be identified straightforwardly. Judging by the interplanar distance (accounting for the limited precision of our measurements) they could be referenced as (001), but they are not perpendicular to the boundaries of the abovementioned areas as (001) in “2”. The angle they compose with these boundaries (parallel to (100) planes) is approximately  $\sim 74^\circ$ .

We propose the following explanation of this contrast. Let us consider the fragments of the WC lattice with zone axes [010] and [001] (see Fig. 6). Let us designate the stacking sequence of the atomic planes (100) in a following way: planes of tungsten atoms by Roman letters (A, B, ...) and the planes of carbon atoms by Greek letters ( $\alpha$ ,  $\beta$ , ...). In this case the fragment with zone axis [010] corresponds to the stacking sequence  $A\alpha A\alpha \dots$  (see the left part of the Fig. 6). A single stacking fault



**Fig. 2.** Black spheres are carbon atoms and gray (green) spheres are tungsten atoms. a) The scheme of a stacking fault in (100) in WC; the stacking fault represents itself a shift of the atomic plane (100) at vector  $1/2 \cdot [011]$ . b) Two parts of WC crystal lattice rotated at  $90^\circ$  one relatively to another. The boundary between these two parts is shown as shaded plane. Such a grain boundary has index  $\Sigma = 2$ , and it can be formed by a stacking fault shown in (a). It can be seen, that the right part of the crystal ([010] zone axis) can be obtained from the left part (zone axis [001]) by consequent shift of each of (100) atomic planes in the direction shown by the arrows in (a). (For interpretation of the references to color in this figure legend, the reader is referred to the web version of this article.)

in this sequence can give rise to a formation of the fragment with zone axis [001] corresponding to the stacking sequence  $A\alpha B\beta\dots$  (central part of the Fig. 6). And two consecutive stacking faults form a structure with stacking  $A\alpha A\alpha B\beta B\beta\dots$ , which is the polytype of WC with a unit cell designated by a dashed rectangle in Fig. 6. In this case the period of high resolution image in the direction [210] of the initial lattice (Fig. 6) will be divisible by  $d_{(100)}$ , whereas the diagonal contrast in the high resolution image is expected to correspond to the interplanar distance  $d_1 = d_{(001)} \cos 16.1^\circ$  and compose an angle  $73.9^\circ$  with (100) atomic planes. This interplanar distance and this angle highly coincide with ones, observed in the areas “3” in the high resolution image in Fig. 5.

In order to confirm our assumption we perform numerical simulation of high resolution image of the polytype lattice. For this we use the following description of the elementary unit cell of the polytype:

$a = b = 0.284 \text{ nm}$ ,  $c = 1.01 \text{ nm}$  ( $c \parallel [210]$ ,  $a \parallel [001]$  direction in the original lattice (see Fig. 6)). The atom set is the following: W (0; 0; 0), W (0; 1/2; 1/4), W (1/2; 1/2; 1/2), W (1/2; 0; 3/4), C (1/2; 1/2; 1/12), C (1/2; 0; 1/3), C (0; 0; 7/12), and C (0; 1/2; 5/6). Thus, this is a tetragonal lattice cell with spatial symmetry group  $I4_1md$  (109). For the simulation we used NCEM simulation program.

Fig. 7a shows enlarged fragment of type “3” area from Fig. 5 (the second area “3” from the right), and Fig. 7b shows simulated image of the corresponding section (zone axis [010]) of the polytype, described above. As it can be seen the contrast on both images practically coincide (experimental image is noisy).

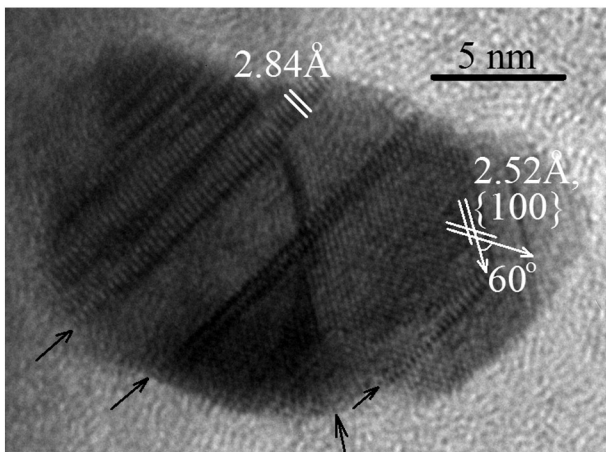


**Fig. 3.** WC nanoparticle. The right part of the particle represents WC lattice with [001] zone axis. Stacking faults parallel to {100} planes are seen in the particle, marked by black arrows in the figure. In the left upper part of the particle there are contrasts corresponding to the atomic planes with interplanar distance of 0.28 nm, which correspond to (001). This planes cannot be seen for the [001] zone axis, so, the band in the left upper part of the particle is WC lattice rotated at  $90^\circ$  relatively to the right lower part. This type of  $\Sigma = 2$  grain boundary was discussed earlier in the literature [9]. In the left upper part there are also other bands with atomic plain contrast which differ slightly from (001). Apparently, they appear in the same way owing to the stacking faults, but are not (001). Their appearance will be discussed further in the text.

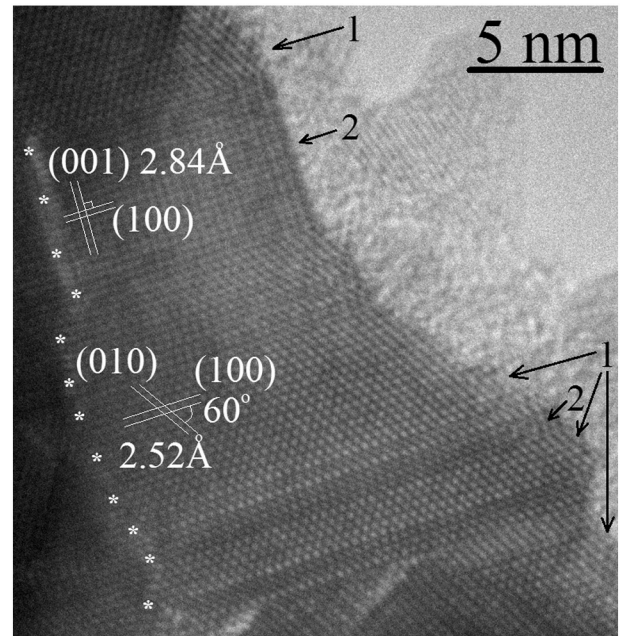


**Fig. 4.** High resolution TEM image of WC particle with stacking faults and differently oriented grains. Areas of type “1” shown by the arrows correspond to the crystal lattice with zone axis [001]. Areas of type “2” correspond to the lattice with zone axis [010]. Boundaries between “1” and “2” have  $\Sigma = 2$ , and combinations of several stacking faults are seen along some of the boundaries. The boundaries marked by white asterisks have higher value of  $\Sigma$ .

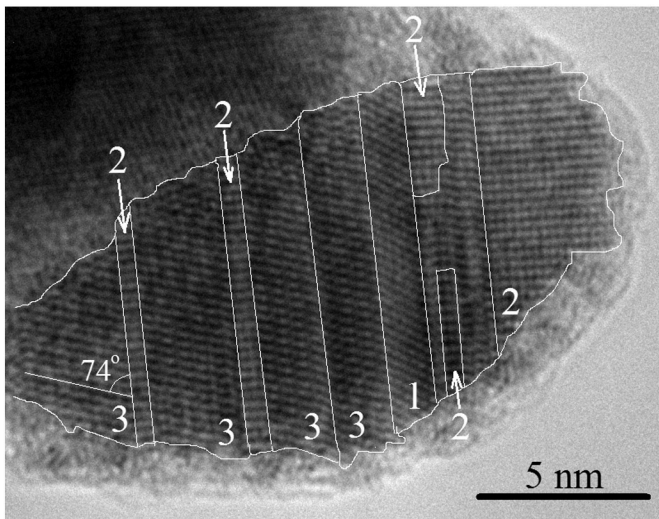


**Fig. 5.** WC nanoparticle with stacking faults separating different fragments of the crystal lattice. These boundaries are highlighted by white lines. Type 1 fragment is WC lattice with zone axis [001]; type 2 fragments have [010] zone axis; type 3 fragments cannot be identified as hexagonal WC lattice and are treated as WC polytype, which is schematically shown in Fig. 6.

Stacking faults in {100} in hexagonal WC are well known in scientific literature [8–10]. In [6,8,9] the structure of such defects (serving as grain boundaries sometimes [9]) was considered thoroughly by high resolution microscopy studies of cemented WC–Co and modeling of high resolution images. It was shown that often defects present in the initial WC nanopowder. In [10] WC was used as a precursor for sintering, and it was shown that such defects can arise due to the thermal stress, which relaxes by creation of stacking faults.

In our case we did not observed such a big amount of defects in the initial pure tungsten powder, as in the sintered sample, and, on the other hand, thermal stress hardly can induce such a big amount of stacking faults to form large fragments of the rotated lattice of WC. We believe that in our sample these stacking faults (along with the lattice

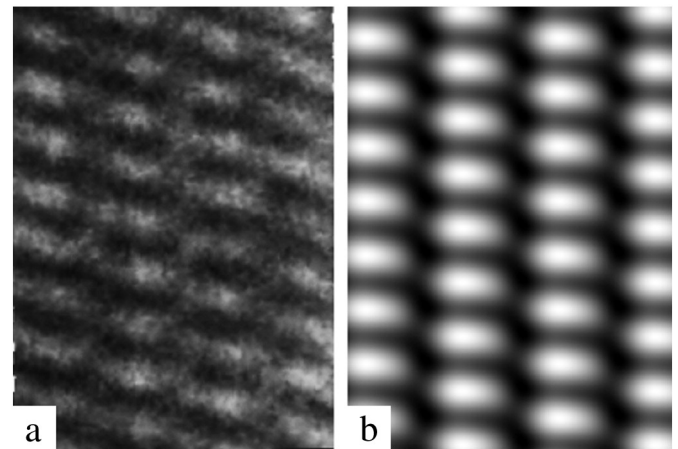


**Fig. 7.** a) Enlarged fragment of type “3” area from Fig. 5; b) simulated high resolution image (NCMS simulation program) of WC polytype with tetragonal lattice (see text) corresponding to [010] zone axis of the polytype, which is parallel to [010] of hexagonal lattice of WC. The following parameters of simulation scheme were used: defocus – 15 nm and thickness 10 nm.

transformation (rotation) and polytype formation) appear at the stage of WC formation during the diffusion of carbon atoms in W.

Probably such a mechanism of lattice transformation can lead to the formation of other polytypes in WC with other stacking sequences. Different stacking sequences will correspond to a range of discrete values of interplanar distances and angles, which the new planes compose with (100) planes. For example, unidentified planes in the left upper part of the particle in Fig. 3, perhaps, can be referred as such polytypes.

## Conclusion

We performed TEM studies of the structure of the sample obtained by sintering tungsten nanopowder with fullerene by the short pulse of the electric current. Synthesized sample consisted of WC nanoparticles with characteristic size from nanometers to tens of

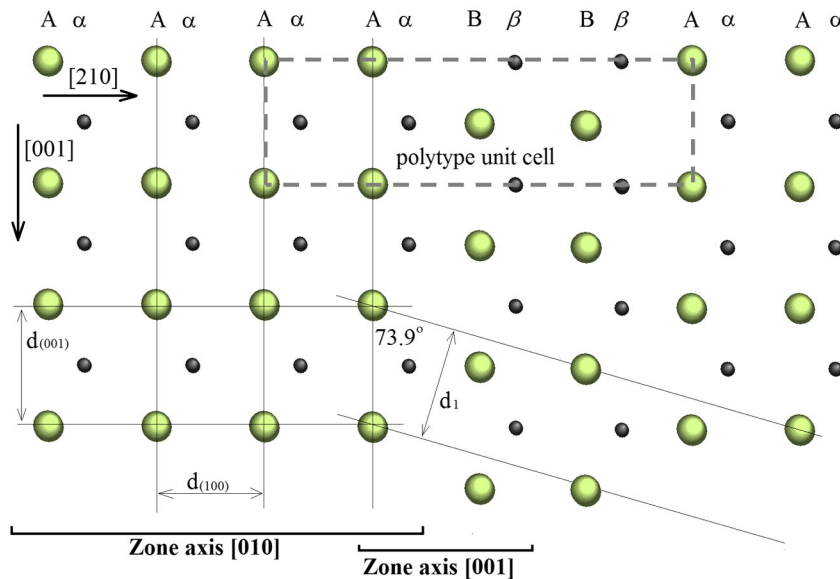


**Fig. 6.** Black spheres are carbon atoms and gray (green) spheres are tungsten atoms. Proposed scheme of the stacking faults in WC explaining the contrast in type “3” fragments in Fig. 5. Left part of the figure corresponds to WC lattice with [010] zone axis. Vertical columns of atoms correspond to (100) atomic planes. Here the stacking of these planes is indicated by Roman and Greek letters in a row above the scheme. Roman letters stand for the planes of tungsten atoms, and Greek letters stand for the planes for carbon atoms. Using this notation, the crystal lattice of WC with [010] zone axis can be referred as  $A\alpha A\alpha\dots$  stacking sequence, the lattice with [001] zone axis corresponds to  $A\alpha B\beta\dots$  stacking sequence, and type 3 areas correspond to  $A\alpha A\alpha B\beta B\beta\dots$  stacking sequence. The contrast in the high resolution image in Fig. 5 in areas 3 apparently corresponds to the planes in this new structure composing  $73.9^\circ$  with (100) atomic planes and having an interplanar distance of  $d_1 = d_{(001)} \cos 16.1^\circ \approx 0.273\text{nm}$ .

nanometers surrounded by the amorphous carbon and closed onion-like curved structures (consisting of few layers). Almost all of the particles in the sample contained stacking faults in (100) planes and some of the particles contained fragments of WC lattice rotated at 90° one relatively to the other, separated by a stacking faults. We also observed the formation of WC polytype (by certain sequence of stacking faults) not reported earlier in literature, and we have proposed a structure (crystal cell) of this polytype.

To all appearances the formation of stacking faults in (100), rotated lattice fragments and the polytypes takes place during the transformation of tungsten to tungsten carbide and peculiarities of carbon diffusion through the tungsten. Therefore, the sintering of W/C<sub>60</sub> mixture (as well, as probably the sintering of pure W nanopowder with other carbon materials) leads to the formation of tungsten carbide with a big amount of different grain boundaries and polytypes, which yield a broad range of the synthesized WC structures.

#### Acknowledgments

This work was supported by the Ministry of Education and Science of Russian Federation within the framework of state contract No.

14.577.21.0090. The research was done using Shared-Use Equipment Center of Technological Institute for Superhard and Novel Carbon Materials.

#### References

- [1] Fernandes CM, Senos AMR. *Int J Refract Met Hard Mater* 2011;29:405–18.
- [2] Sommer M, Schubert W-D, Zobetz E, Warbichler P. *Int J Refract Met Hard Mater* 2002;20:41–50.
- [3] Fang ZZ, Wang X, Ryu T, Hwang KS, Sohn HY. *Int J Refract Met Hard Mater* 2009;27: 288–99.
- [4] Blank V, Popov M, Buga S, Davydov V, Denisov V, Ivlev A, et al. *Phys Lett A* 1994;188: 281–6.
- [5] Bonache V, Salvador MD, Busquets D, Burguete P, Martínez E, Sapiña F, et al. *Int J Refract Met Hard Mater* 2011;29:78–84.
- [6] Lay S, Loubradou M, Schubert W-D. *J Am Ceram Soc* 2006;89:3229–34.
- [7] Kurlov AS. *Russ J Phys Chem A* 2013;87:654–61.
- [8] Lay S. *Int J Refract Met Hard Mater* 2013;21:416–21.
- [9] Lay S, Loubradou M. *Philosophical Magazine* 2003;83:2669–79.
- [10] Wu XY, Zhang W, Li DX, Guo JD. *Mater Sci Technol* 2007;23:627–9.